Addition of granular activated carbon and trace elements to favor volatile fatty acid consumption during anaerobic digestion of food waste

Gabriel Capson-Tojo, Roman Moscoviz, Diane Ruiz, Gaelle Santa-Catalina, Eric Trably, Maxime Rouez, Marion Crest, Jean-Philippe Steyer, Nicolas Bernet, Jean-Philippe Delgenès, et al.

Addition of granular activated carbon and trace elements to favor volatile fatty acid consumption during anaerobic digestion of food waste

Gabriel Capson-Tojo, Roman Moscoviz, Diane Ruiz, Gaëlle Santa-Catalina, Eric Trably, Maxime Rouez, Marion Crest, Jean-Philippe Steyer, Nicolas Bernet, Jean-Philippe Delgenès, Renaud Escudié

PII: S0960-8524(18)30459-0
DOI: https://doi.org/10.1016/j.biortech.2018.03.097
Reference: BITE 19736

To appear in: *Bioresource Technology*

Received Date: 24 February 2018
Revised Date: 16 March 2018
Accepted Date: 19 March 2018

Please cite this article as: Capson-Tojo, G., Moscoviz, R., Ruiz, D., Santa-Catalina, G., Trably, E., Rouez, M., Crest, M., Steyer, J-P., Bernet, N., Delgenès, J-P., Escudié, R., Addition of granular activated carbon and trace elements to favor volatile fatty acid consumption during anaerobic digestion of food waste, *Bioresource Technology* (2018), doi: https://doi.org/10.1016/j.biortech.2018.03.097

Addition of granular activated carbon and trace elements to favor volatile fatty acid consumption during anaerobic digestion of food waste

Gabriel Capson-Tojo [a,b], Roman Moscoviz [a], Diane Ruiz [a], Gaëlle Santa-Catalina [a], Eric Trably [a], Maxime Rouez [b], Marion Crest [b], Jean-Philippe Steyer [a], Nicolas Bernet [a], Jean-Philippe Delgenès [a], Renaud Escudié [a,*]

[a] LBE, INRA, Univ. Montpellier, 102 avenue des Etangs, 11100, Narbonne, France

[b] Suez, CIRSEE, 38 rue du Président Wilson, 78230, Le Pecq, France

[*] Corresponding author: tel. +33 (0) 468.425.173, e-mail: *renaud.escudie@inra.fr*

Abstract

The effect of supplementing granular activated carbon and trace elements on the anaerobic digestion performance of consecutive batch reactors treating food waste was investigated. The results from the first batch suggest that addition of activated carbon favored biomass acclimation, improving acetic acid consumption and enhancing methane production. Adding trace elements allowed a faster consumption of propionic acid. A second batch proved that a synergy existed when activated carbon and trace elements were supplemented simultaneously. The degradation kinetics of propionate oxidation were particularly improved, reducing significantly the batch duration and improving the average methane productivities. Addition of activated carbon favored the growth of archaea and syntrophic bacteria, suggesting that interactions between these microorganisms were enhanced. Interestingly, microbial analyses showed that hydrogenotrophic methanogens were predominant. This study shows for the first time that addition of granular activated carbon and trace elements may be a feasible solution to stabilize food waste anaerobic digestion.

Keywords

Biomethane; DIET; biomass acclimation; ammonia; environmental biorefinery

1. Introduction

The production of food waste (FW) is a global issue and a huge effort is currently being put to reduce the amounts of FW generated and to develop new sustainable technologies for its treatment. Among all the possible processes for FW treatment, anaerobic digestion (AD) stands as an environmental-friendly alternative that offers a triple role: (i) waste stabilization, (ii) C-recovery via production of renewable energy in the form of biogas and (iii) nutrient (*e.g.* N, P and K) recovery by digestate application. Thus, within the concepts of circular economy and sustainable industry, AD is clearly an interesting process. Moreover, international regulations (European Directive 2008/98/CE) imposing the valorization of commercial FW from gross producers through soil return for both C and nutrient recovery are recently being applied, precluding traditional/obsolete methods such as landfilling or incineration.

However, AD of highly concentrated substrates such as FW (20 % total solids; TS) is a complex biological process prone to failure if it is not properly managed. As FW is mainly composed of easily degradable carbohydrates, the reactor can be easily overloaded, leading to accumulation of volatile fatty acids (VFAs) due to unbalance of the acidogenesis/acetogenesis and methanogenesis steps (Capson-Tojo et al., 2016). Another issue occurring during FW AD is related to the high protein content of this substrate, which eventually leads to high concentration of total ammonia nitrogen (TAN) in the reactors. Therefore, long term continuous AD experiments have reported high concentrations of free ammonia nitrogen

(FAN), which is toxic to microorganisms (Banks et al., 2008; Capson-Tojo et al., 2017b; Rajagopal et al., 2013). Acetoclastic methanogens are particularly sensitive to high TAN/FAN concentrations (TAN over 2.8-3.0 $g \cdot l^{-1}$). Because of this, hydrogenotrophic and mixotrophic archaea (more resistant to TAN/FAN inhibition and VFA peaks) have been found to be predominant species at high TAN concentrations (Jiang et al., 2017). As a consequence, it has been stated that syntrophic acetate oxidation (SAO; Eq. 1) and hydrogenotrophic methanogenesis (HM; Eq. 3) are predominant pathways for methane production during AD of FW (Banks et al., 2012; Capson-Tojo et al., 2017c). During this processes, syntrophic interactions between bacteria and archaea are crucial to avoid accumulation of intermediate metabolites such as VFAs, molecular hydrogen or formic acid in the reactors. If these compounds accumulate, it leads to acidification of the process, decreasing the pH to values where methane production is stopped.

Syntrophic acetate oxidation (SAO):

$$CH_3COO^- + 4H_2O \rightarrow 2HCO_3^- + H^+ + 4H_{2\,(g)} \qquad \Delta G'^\circ = +\,104\ kJ \cdot mol^{-1} \qquad \text{Eq. 1}$$

Syntrophic propionate oxidation (SPO):

$$CH_3CH_2COO^- + 2H_2O \rightarrow CH_3COO^- + HCO_3^- + H^+ + 3H_{2\,(g)} \qquad \Delta G'^\circ = +\,76.1\ kJ \cdot mol^{-1} \qquad \text{Eq. 2}$$

Hydrogenotrophic methanogenesis (HM):

$$4H_{2\,(g)} + HCO_3^- + H^+ \rightarrow CH_{4\,(g)} + 3H_2O \qquad \Delta G'^\circ = -\,132\ kJ \cdot mol^{-1} \qquad \text{Eq. 3}$$

Acetoclastic methanogenesis:

$$CH_3COO^- + H_2O \rightarrow CH_{4\,(g)} + HCO_3^- \qquad \Delta G'^\circ = -\,31.0\ kJ \cdot mol^{-1} \qquad \text{Eq. 4}$$

During HM, hydrogen and formic acid act as sole electron shuttles for methane production, allowing mediated interspecies electron transfer (MIET) to occur (Lovley, 2017). Therefore,

the balance between the production-consumption processes of these shuttles is much more relevant in HM when compared with acetoclastic methanogenesis (Eq. 4). Propionic acid (HPr) has been reported to be particularly problematic, getting easily accumulated during FW AD and causing inefficient AD and eventually process failure (Banks et al., 2011, 2008, Capson-Tojo et al., 2017a, 2017b, 2016; Zhang et al., 2015a). As explained in Capson-Tojo et al. (2017a) and Batstone et al. (2002), this occurs because syntrophic propionate oxidation (SPO; Eq. 2) becomes rapidly thermodynamically unfavorable when main AD intermediates such as acetic acid (HAc), molecular hydrogen or formic acid start to accumulate. Thus, the build-up or these metabolites during HM explains why HPr and HAc accumulate frequently during FW AD.

If VFA accumulation is to be avoided during FW AD, the kinetics of SPO must be improved, by promoting the growth of HPr oxidizers and/or favoring the consumption of hydrogen/formate and HAc (promoting SAO), thus making SPO thermodynamically feasible. The main approach that has been addressed in the literature to avoid HPr accumulation during FW AD is the addition of trace elements (TEs), which are known to enhance degradation rates in AD (Banks et al., 2012; Voelklein et al., 2017; Zhang et al., 2015b). As previous research suggests, the synthesis of enzymes is of critical importance during syntrophic HM, particularly for the production of formate dehydrogenase for formate cleavage (Banks et al., 2012). This process requires TEs, such as iron, selenium, cobalt, molybdenum, nickel or tungsten, which have been found to stabilize both mesophilic and thermophilic AD of FW (Banks et al., 2012; Qiang et al., 2013, 2012; Zhang et al., 2015a). The concentrations of those in FW is not sufficient and therefore the supplementation of mixtures of TEs has effectively avoided the accumulation of VFAs at high organic loading rates (OLRs) (Zhang et

al., 2011; Zhang et al., 2015b; Zhang et al., 2015a) and some studies have even shown that it is possible to recover acidified reactors using TEs (Qiang et al., 2013, 2012).

Another possibility that is currently receiving a lot of attention to favor VFA consumption during AD is the addition of carbon-based conductive materials (Dang et al., 2016), such as granular activated carbon (GAC). Other than favoring the adsorption of inhibitors and allowing the formation of biofilms onto their surface, it has been suggested that these materials can improve syntrophic interactions between microorganisms (Fagbohungbe et al., 2017). Due to their relatively high electrical conductivity and their particular surface chemistry, they can serve as electron acceptor during AD and, once reduced, they are also able to act as electron donor (Liu et al., 2012). Therefore, GAC has been found to permit direct interspecies electron transfer (DIET) to occur on their surface (Dang et al., 2016). DIET is an alternative to MIET in which the electrons are transferred between the electron-donating and -accepting partners through electrical connections, which can be formed by conductive pili, electron transport proteins or electrically conductive materials (Lovley, 2017). When compared to MIET, DIET is expected to be a faster and more efficient mechanism of electron transfer (Cruz Viggi et al., 2014; Lovley, 2017). In addition, as during DIET electron shuttles (such as hydrogen or formate) are no longer formed, the degradation of VFAs during AD is thermodynamically independent of the concentrations of these species (Dang et al., 2016; Lee et al., 2016). Thus, the application of these materials to favor DIET and avoid VFA accumulation during AD of complex-concentrated substrates (such as FW) appears as an alternative with a huge potential.

The objective of this study was to evaluate for the first time the effect of GAC and TEs addition on the AD performance using consecutive batch reactors fed with FW. Particular

attention was paid to the VFA accumulation/consumption kinetics and to the evolution of the microbial communities.

2. Materials and methods

2.1. Inoculum and substrate

The inoculum used to start the reactors was collected from an industrial plant treating different organic streams at high TAN/FAN concentrations (5.04 g TAN·l^{-1}; 615 mg FAN·l^{-1}). This inoculum was selected because it was assumed that the microbial population would already be adapted to high FAN concentrations, like those existing during FW AD. The inoculum had an initial TS content of 5.81±0.02 %, with 59.1±0.1 % corresponding to volatile solids (VS). It must also be mentioned that, while some TEs were already present in the inoculum (*i.e.* 18 g Fe·kg TS^{-1}, 163 mg Cu·kg TS^{-1}, 643 mg Mn·kg TS^{-1} and 649 mg Zn·kg TS^{-1}), others were not detected (*i.e.* Co).

The FW was collected from different producers from the region of the Grand Narbonne, in the south of France. A proportional mixture (wet weight) of the different FWs was used as substrate. With TS contents of 21.0 % (90.3 % VS), being mainly composed of carbohydrates (618 g·kg TS^{-1}), followed by proteins (187 g·kg TS^{-1}) and lipids (121 g·kg TS^{-1}) and with relatively low C/N ratios (16.1), the results for the mixed FW were in agreement with typical values presented in the literature (Capson-Tojo et al., 2016). The obtained values also confirmed the low concentrations of some TEs in FW, such as Co (< 9.75 mg·kg TS^{-1}), Mo (1.26 mg·kg TS^{-1}) or Ni (1.19 mg·kg TS^{-1}). Interestingly, high concentrations of Fe were found (1114 mg·kg TS^{-1}). A deeper discussion of these results as well as a more extensive characterization can be found in Capson-Tojo et al. (2017a).

2.2. Consecutive batch anaerobic digestion

All the batch reactors were started using 60 g of FW as substrate (raw). The substrate to inoculum (S/X) ratio was set as 1 g VS·g VS^{-1}, which led to FW concentrations of approximately 30 g VS FW·l^{-1}. An amount of 368 g of inoculum was then added in each reactor. The reactors were incubated at 37 °C and had an initial working volume of 430 ± 2 ml. The Control reactor was fed with only FW. The TEs reactor had equivalent working conditions but was supplemented with TEs at the following concentrations: 100 mg·l^{-1} Fe, 1 mg·l^{-1} Co, 5 mg·l^{-1} Mo, 5 mg·l^{-1} Ni, 0.2 mg·l^{-1} Se, 0.2 mg·l^{-1} Zn, 0.1 mg·l^{-1} Cu, 1 mg·l^{-1} Mn. These values were estimated from optimal results reported in the literature (Banks et al., 2012; Zhang et al., 2015b). The required volume of a concentrated solution (x100) containing $FeCl_2 \cdot 4H_2O$, $CoCl_2 \cdot 6H_2O$, $Na_2MoO_4 \cdot 2H_2O$, $NiCl_2 \cdot 6H_2O$, Na_2SeO_3, $ZnCl_2 \cdot 2H_2O$, $CuCl_2 \cdot 2H_2O$, $MnCl_2 \cdot 4H_2O$ was used for doping the reactor. Similarly, GAC at a concentration of 10 g·l^{-1} was added to the GAC reactor. The initial concentration of GAC was defined according to Lee et al. (2016). Finally, the reactor GAC + TEs was supplemented simultaneously with the same concentrations of TEs and GAC used above. The GAC was supplied by Sigma-Aldrich (Missouri, United States of America; CAS 7440-44-0). The incubation system was an Automated Methane Potential Testing System (AMPTSII) (Bioprocess Control, Sweden). The AMPTSII system consisted of 12 parallel reactors with a total volume of 500 ml and connected to CO_2 traps (NaOH solutions) and to gas flow meters to determine continuously the methane flow rate. The AMPTSII agitated the reaction media during 1 minute every 10 minutes at 40 rpm. Other than providing an automatic measurement of the biogas produced, this system has the advantage of allowing an easy sampling of the digestate, through a hole present in each reactor than can be used as sampling port. Thus, the follow-up of the dynamics of VFA accumulation was facilitated. All the conditions were run in triplicate. In order to account for inoculum adaptation, a second feeding was performed at

the same conditions applied in the first one (S/X ratio of 1 g VS·g VS^{-1}). The reactors containing TEs or GAC were further supplemented in these reactants/materials according to the amount of digestate removed after the first batch and to the amount of raw FW added as substrate for the second batch. Consecutive batch reactors were used because of two main reasons: (i) they allow testing different conditions simultaneously and (ii) the results can be extrapolated to large scale plug-flow reactors operating with digestate recirculation. In addition, batch reactors are widely used for solid waste valorization and will play a main role in future biorefineries for FW valorization (Sadhukhan et al. 2014, Capson-Tojo et al. 2016). It is important to mention that recent consecutive batch studies have shown that HPr is degraded much slower than the other VFAs. Therefore, even if the accumulated HPr might not account for a high percentage of the final methane yields, if the batch does not last enough time to allow HPr oxidation, this VFA will accumulate after each reactor feeding, eventually leading to reactor acidification (Capson-Tojo et al., 2017b). Thus, HPr degradation defines the batch duration. Consequently, the reactors were fed after 34 days, when a biogas plateau existed and the HPr had been consumed.

Before presenting the results, it must be commented that in the first batch another GAC supplemented reactor was carried out. In this case, other than GAC, *Geobacter sulfurreducens* was also added into the reactors. This microorganism is a well-known DIET performer and is also known to grow attached onto GAC particles (Liu et al., 2012). The results from these reactors (GAC + Geo) were identical to those observed in the GAC reactors, meaning that the addition of *Geobacter* did not enhance the VFA degradation kinetics. Therefore, this *Geobacter*-inoculated reactor was stopped after the first feeding and, in the second batch, these GAC-containing reactors were supplemented with TEs (at the same concentration

applied in the TEs reactors): this new condition was used to elucidate the effect of the simultaneous addition of both AD enhancers (GAC+TEs).

2.3. Analytical methods

2.3.1. Physicochemical characterization of the FW

The FW was extensively characterized (Capson-Tojo et al., 2017b). TS and VS contents were determined according to the standard methods of the American Public Health Association (APHA, 2005). The concentration of carbohydrates was measured using the Dubois method (Dubois et al., 1956). The content of lipids was determined by a gravimetric method based on accelerated solvent extraction using an ASE®200, DIONEX (California, United States of America) coupled to a MULTIVAPOR P-12, BUCHI (Aquon, Netherlands) with heptane as solvent (100 bar, 105 °C, 5 cycles of 10 min static and 100s purge) (APHA, 2005). Total Kjeldahl nitrogen (TKN) and NH_4^+ concentrations were measured with an AutoKjehdahl Unit K-370, BUCHI. The concentration of proteins was estimated from the TKN contents (6.25 g protein·g N^{-1} (Jimenez et al., 2013)). Total organic carbon (TOC) and inorganic carbon (IC) were determined using a Shimadzu (Kyoto, Japan) TOC-V_{CSN} Total Organic Carbon Analyzer coupled to a Shimadzu ASI-V tube rack. The total carbon (TC) was calculated as the sum of TOC and IC. The C/N ratio was calculated as TC/(TKN+TAN). The pH was measured by a WTW (London, United Kingdom) pHmeter series inoLab pH720. The BMPs of the substrates were determined according to Motte et al. (2014). The conversion of chemical oxygen demand (COD) was calculated according to the input COD from the substrates and that found as products (methane and VFAs) after AD. The COD of the FW was estimated from the contents in carbohydrates (1.067 g COD·g^{-1}), proteins (1.57 g COD·g^{-1}) and lipids (2.87 g COD·g^{-1}) (Batstone et al., 2002).

The concentrations of micro-elements were determined by Aurea Agroscience© (Ardon,

France). The contents on metallic trace elements were measured by water extraction, according to the norm NF EN 13346. The concentrations of Fe, Cu, Ni, Mn, Mo, Co and Zn were measured by plasma emission spectrometry, according to the NF EN ISO 11885.

2.3.2. Analysis of metabolites and final products

A plastic tube submerged in the sludge and connected to the cover of the AMPTSII reactors enabled sampling of digestate without modifying the composition of the gas in the headspace. Before sampling, the gas output was blocked and the equivalent volume of digestate to be removed was added as nitrogen gas (with negligible effect in the gas composition), avoiding this way an overestimation of the gas produced. Once sampled, the concentrations of VFAs and ionic species in the digestates were measured by gas and ion chromatography, as described in Motte et al. (2013).

2.3.3. Methane quantification

As aforementioned, the reactors of the AMPTSII system were connected to CO_2 traps and to gas flow meters that measured continuously the methane flow rate. To account for the endogenous respiration from the inoculum, blank reactors were carried out (in triplicate) and the corresponding methane production was subtracted from that of the reactors.

2.4. qPCR and MiSeq sequencing analysis

To study the evolution of the microbial communities during the AD process, four sampling points were selected from the first batch process. In addition, as the endogenous microbial communities present in the FW are known to have a significant effect on its characteristics (mainly due to pre-degradation during FW storage) (Fisgativa et al., 2017), samples of the FW and the initial inoculum were analyzed separately.

Real-time polymerase chain reaction (qPCR) and DNA sequencing techniques were used to analyze the samples.

To evaluate the growth or decay of a microbial population, the number of times the population was doubled (N_g; growth rate) was calculated by:

$$N_g = \frac{\ln(\frac{X_f}{X_i})}{\ln(2)} = \log_2(\frac{X_f}{X_i}) \quad \text{Eq.5}$$

Where X_i and X_f are the initial and final concentrations of 16 S copies respectively.

The qPCR measurements of each sample were performed in triplicate to assess the technical standard error associated with the measurement (σ). The raw qPCR results were $\log_2$ transformed and the variance between replicates was used to calculate the standard error of measurement. Values of 0.53 and 0.43 $\log_2$(16 S copies·g^{-1}) were found for bacteria and archaea, respectively. It was considered that no growth (or decay) existed when values of N_g lower than twice σ (1.05 and 0.87 $\log_2$(16 S copies·g^{-1}) for bacteria and archaea) were observed.

A precise description of the methodology employed can be found elsewhere (Moscoviz et al., 2017).

2.5. Data analysis

The methane yields were calculated by dividing the total volume of methane produced by the initial mass of VS of substrates. The yields were corrected to account for the digestate removed. The concentration of FAN was calculated according to Rajagopal et al. (2013) as a function of temperature, pH, ionic strength and TAN concentration. The concentrations of the main ions present in the reactors (Cl^-, Na^+, NH_4^+, K^+, Mg^{2+}, H^+ and Ca^{2+}) were taken into account in this calculation.

3. Results and discussion

3.1. Performance of the consecutive batch reactors

As aforementioned, the batch reactors were fed twice consecutively. During the first batch (with an S/X ratio of 1 g VS·g VS^{-1}; 30 g VS FW·l^{-1}), three different conditions were monitored: a Control reactor, a reactor supplemented with TEs and a reactor supplemented with GAC. The reactors lasted for 34 days and during this period 15 samples were taken to analyze the composition of the reacting medium. Figure 1 presents the methane yields, the total products measured and the concentrations of the main VFAs (acetic acid, propionic acid, butyric acid and valeric acid).

As it can be observed, methane was produced efficiently, but a lag phase on the methane production existed in all the reactors. These lag periods were likely caused by the initial accumulations of VFAs (mainly HAc and HPr, with traces of HBu and valeric acid). However, while lag phases of around 10 days existed in the Control and TEs reactor, the lag period in GAC lasted only for 2 days. This occurred because the addition of GAC promoted the early consumption of HAc (Figure 1C), with concentrations up to 9.9 g·l^{-1} in the GAC reactor and up to 15.4 g·l^{-1} in the Control reactor. In addition, while in the GAC reactor the HAc concentrations after 15 days were already low (0.6 g·l^{-1}), it was necessary to wait until day 24 to achieve these values in the TEs reactor and until day 27 in the Control. The faster substrate conversion is also suggested by Figure 1B (total products as sum of methane plus VFAs in COD units), where it can be observed that the GAC reactors achieved high substrate conversion before the other conditions.

Table 1 shows the corresponding maximum methane production rates (397-419 ml·d^{-1}), the maximum rates of HAc and HPr consumption (1.59-1.76 g·l^{-1}·d^{-1} and 0.32-0.58 g·l^{-1}·d^{-1}, respectively) and the final COD recoveries (81.9-87.9 %). Interestingly, the values of the maximum HAc consumption rates shown in Table 1 were not significantly different (1.59-1.76 g·l^{-1}·d^{-1}), suggesting that the favored methane production (and concomitant HAc

consumption) in the GAC reactor was mainly related to a favored initial growth of the microorganisms but that, once growing, the AD kinetics (in exponential growth) were similar independently of the initial lag phase observed. In addition, when looking at the maximum methane production rates, it can be observed that they were not significantly different between the reactors (397-419 $ml \cdot d^{-1}$). Summarizing, it can be concluded that GAC addition favored biomass acclimation during this first feeding, reducing the observed lag phases. Interestingly, even if GAC supplementation improved HAc degradation, this was not translated into a more efficient HPr consumption. As shown in Figure1D, the degradation of HPr did not start until day 22 in all the reactors and it was not finished until days 31 (TEs) and 34 (GAC). This suggests that HPr oxidation was not only limited thermodynamically (due to high concentrations of metabolites in the media), but also by the absence of HPr-degrading microorganisms. However, the addition of TEs showed the highest maximum HPr degradation rate (up to 0.58 $g \cdot l^{-1} \cdot d^{-1}$) and the lowest time for total HPr (31 days; Table 1), which suggested a positive effect of their supplementation. Concerning the consumption of HBu and valeric acid (HVal), the GAC reactor showed also the best performances, with lower maximum concentrations achieved (Figure 1E and Figure 1F) and lower times required for their total degradation (Table 1). This suggests that GAC addition also favored the consumption of these VFAs.

Once the first batch was finished, the reactors were fed again with an S/X ratio of 1 g VS·g VS^{-1} (30 g VS $FW \cdot l^{-1}$). In this case, four different conditions were monitored: a Control reactor, a reactor supplemented with TEs, a reactor supplemented with GAC and a reactor supplement with both TEs and GAC (to assess the simultaneous effect of these reactants). The batches lasted for 31 days and again 15 samples were taken to analyze the composition of the reacting medium. The corresponding methane yields, methane production rates and the

concentrations of the main VFAs (HAc, HPr, HBu and HVal) are shown in Figure 2. As for the first batch, the maximum methane production rates, COD recoveries, final pH values, maximum consumptions rates of acetic and propionic acids and the times required for total VFA consumption are also presented in Table 1.

The global behavior was totally different between both feeding cycles. In the second batch no lag phases in the methane production were observed in any condition and HAc (in this case only up to 9.3 $g \cdot l^{-1}$) started to be degraded after only two days in all the reactors. Moreover, similar kinetics of HAc production-consumption (as well as total COD conversions) were observed in all the reactors. This indicates that the first batch served mainly for biomass growth and acclimation, processes that were favored by adding GAC. When comparing the results presented in Figure 1, Figure 2 and Table 1 for the two consecutive feedings, it can be appreciated that, while the methane yields did not differ much between the consecutive batches (410-443 and 443-452 ml $CH_4 \cdot g\ VS^{-1}$, respectively), the maximum methane production rates were much higher in the second one, with values of 545-719 $ml \cdot d^{-1}$ (*vs.* 397-419 $ml \cdot d^{-1}$ in the first feeding). This value was particularly improved in the reactors supplemented with GAC, with the maximum rate obtained in the GAC+TEs reactor (719 $ml \cdot d^{-1}$). Moreover, it can be observed in Table 1 that the times required to achieve a total consumption of the accumulated VFAs were also much lower in the second feeding (*i.e.* 27 days *vs.* 10 days for HAc consumption in the Control reactor). These results indicate that biomass acclimation after the first batch clearly improved the methane production kinetics and the VFA degradation in all conditions. This suggests that biomass acclimation must always be considered when performing batch studies and, particularly, if concentrated substrates known to induce microbial selection in digesters (such as FW) are used (Capson-Tojo et al., 2017c).

The main difference between the GAC supplemented reactors and the other conditions in the second batch can be deducted from Figure 2D and Table 1: the concentrations of HPr and the times required for its total consumption were much lower in the reactors containing GAC. Again, the GAC+TEs system showed the best performance, with HPr concentrations only up to 1.97 $g \cdot l^{-1}$ (*vs.* 3.94 $g \cdot l^{-1}$ in the Control reactor) and without traces of HPr after day 15 (a value which was 22, 31 and over 31 for the GAC, TEs and Control reactors, respectively). Therefore, it can be concluded that, even if the kinetics of methane production and the methane yields were similar in all the reactors, the addition of GAC clearly favored the consumption of the accumulated HPr (avoiding at the same time the extent of its build-up). In addition, a further improvement in the HPr degradation was observed when adding TEs into the GAC-supplemented reactors.

As it has already been suggested in Capson-Tojo et al. (2017a), if the batch reactors are reloaded before the HPr degradation is finished, this compound accumulates sequentially, eventually causing acidification of the reactors and inhibition of the methane production process. Thus, if a stable AD process is to be achieved, the time required for total HPr consumption will determine the batch duration, even if the desired methane yields are reached before consuming all the HPr produced. This implies that the reduction of the time required for total HPr degradation when adding GAC + TEs (from over 30 days in the Control to 15 days) leads to an AD process that can potentially treat efficiently the same amount of FW in less than half of the time. This implies that the average daily methane productivities (calculated as total methane production divided by batch duration) are doubled (*i.e.* 172 vs. 348 ml $CH_4 \cdot l^{-1}$ in the Control and the GAC+TEs reactors, respectively). This improvement is crucial to render an industrial process feasible from an economic point of view. Basically, a decrease of the batch duration has two main consequences, both critical in industrial AD

processes: an increased volumetric methane production rate and an increased treatment capacity.

It must also be mentioned that, besides the high transient VFA concentrations achieved during both feedings, the reactors were not acidified because the high TAN concentrations (10.0-11.1 $g \cdot l^{-1}$; see Table 2) acted as pH buffer, keeping the pH at high values, always above 7.20 regardless the VFA concentration and with final values of 8.03-8.13 (Table 1).

The obtained results were further verified by a third feeding cycle at a higher substrate load (two-fold; ~ 55 g VS $FW \cdot l^{-1}$), where the same four conditions tested in the second feeding were carried out. The results confirmed the synergetic effect of GAC and TEs, with the highest methane production rates and volumetric productivities.

In order to understand the obtained results and to elucidate which microorganisms were dominant, an extensive analysis of the microbial communities was carried out, comparing the different conditions and analyzing the evolution of the populations throughout the first batch.

3.2. Evolution of the microbial communities in the reactors

As aforementioned, four different samples were taken during the first batch (in days 6, 13, 24 and 34). The corresponding sequencing and qPCR results are presented in Figure 3.

Starting with the archaeal populations, the predominant species were similar in all the reactors. In agreement with the literature dealing with AD at high TAN/FAN contents, all the species presented in Figure 3 are hydrogenotrophic methanogens, with no traces of *Methanosaeta* sp. being detected (Capson-Tojo et al., 2017c; Jiang et al., 2017). Considering that the inoculum comes from an AD plant working at high TAN/FAN concentrations (5.04 g $TAN \cdot l^{-1}$) and that these concentrations were even higher after the batches carried out, this is a logical outcome. In addition, other than *Methanosarcina* sp. (which is a mixotrophic microorganism), all the other archaea were strict hydrogen utilizers, indicating that syntrophic

VFA oxidation and HM were the main pathways for methane production. The predominant archaea were *Methanothermobacter* sp. (100 % of 16s rRNA sequence similarity with *Methanothermobacter tenebrarum*) in all the conditions, followed by *Methanobrevibacter* sp. (97 % of 16s rRNA sequence similarity with *Methanobrevibacter acididurans*) and *Methanoculleus* sp. (99 % of 16s rRNA sequence similarity with *Methanoculleus bourgensis*). All these species are known to be thermo-tolerant archaea (with some also identified as halotolerant) (Maus et al., 2012; Nakamura et al., 2013; Savant et al., 2002). This indicates that, at the high transient VFA peaks and TAN/FAN concentrations in the reactors (see Table 2), common acetotrophic archaea (*i.e. Methanosaeta*) were inhibited, and only the most resistant methanogens were able to thrive. It is also interesting to mention a general trend can be observed in the archaeal population dynamics when looking at the qPCR results: after a significant growth during the first week, a sudden decay existed, particularly in the Control and TEs reactors, which was followed by a final, less pronounced, archaeal growth. The periods of growth can be attributed to the presence of VFAs and hydrogen at the beginning of the batch process (from FW degradation) and to the HPr degradation at the end, which were used as substrate for methane production after their conversion by bacteria. Interestingly, the GAC reactor sustained the growth of archaea for a longer period than the other two conditions and the concentrations of archaea after AD were higher in those reactors than in the others, reducing the extent of the aforementioned decay. This suggests that the formation of biofilm onto the GAC particles may have favored archaeal survival. In addition, a more diverse archaeal population was observed in the GAC reactor at the end of the batch, with a Shannon index of 1.55 ± 0.10 (*vs.* 1.25 ± 0.09 and 1.30 ± 0.04 for the Control and TEs reactors, respectively). The presence of *Methanosarcina* (known to participate in DIET (Rotaru et al., 2014b)) was particularly higher in this condition when compared to the Control and TEs

reactors, suggesting that GAC may have favored its growth.

When looking at the bacterial communities (expressed at order level to favor data analysis), it can be observed that, while *Lactobacillales* (mainly lactic acid-producing bacteria similar to *Lactobacillus plantarum*) were predominant in the FW, *Bacteroidales* and *Clostridiales* were the main microorganisms in all the AD reactors. As these microorganisms are known to participate in the processes of hydrolysis and acidogenesis, respectively, their growth during substrate degradation is a logical outcome. As for archaea, after the day 13 the number of microorganisms decreased rapidly. Several reasons might explain this biomass decay, such as endogenous growth due to lack of substrate or the presence of predators or bacteriophages in the media. Again, this decay was much lower in the GAC-doped reactor, suggesting that GAC allowed keeping higher concentrations of alive bacteria in the media.

In an attempt to elucidate the reasons behind this biomass decay and to further understand the positive effect of GAC addition, the growth rates of the main bacterial OTUs were calculated according to Equation 5. The obtained results are presented in Figure 4.

The results show that all the reactors followed a similar trend: an initial growth related to FW degradation was observed, followed by a less pronounced growth and a final biomass decay. As mentioned previously, *Bacteroidales* and *Clostridiales* were the main microorganisms in all the reactors. Their initial growth was related to hydrolysis and acidogenesis from FW as initial AD steps. Interestingly, among the main fermenter bacterial species, numerous syntrophic organisms were detected, such as OTU 7 (belonging to the *Gelria* genus) and OTUs 9 and 10 (*Syntrophomonadaceae* family). This further suggests the importance of these processes during FW AD.

When comparing the performances of the reactors, the main conclusion that can be drawn is again related to the influence of GAC addition. While the Control and the TEs reactors

showed similar population dynamics, with no significant bacterial growth after day 13, the GAC supplemented reactor showed a continuous growth of *Clostridiales* (OTUs 6 and 10) between days 13 to 35. In the case of OTU 6, it is a bacterium known to degrade different sugars and aminoacids to produce HAc and hydrogen (Wu et al., 2010). It belongs to the *Alkaliphilus* genus (96 % of 16S rRNA sequence similarity with *Alkaliphilus halophilus*) and its predominance was probably favored due to the high pH (≥ 8.03) and ionic strength (≥ 0.45) of the media. Regarding OTU 10, it belongs to the *Syntrophomonas* genus (98 % of 16S rRNA sequence similarity with *Syntrophomonas sapovorans*; known syntrophic oxidizing fatty acids of 4-18 carbons when growing with a hydrogen utilizing partner (Roy et al., 1986)). The favored growth of these microorganisms in the presence of GAC further suggests that this material enhanced syntrophic interactions. This can potentially explain the improvement of the HAc and HPr degradation kinetics in the reactors containing GAC particles.

It is interesting to mention that, contrary to what was expected, no known electro-active bacteria (*i.e. Geobacter* sp.) were detected in the reactors at significant concentrations. This implies that (i) either DIET did not occur significantly in the reactors or (ii) DIET was performed by microorganisms not yet known to be capable of performing it. It must be commented that the harsh conditions during FW AD (*i.e.* high TAN/FAN concentrations, high pH, high ionic strength and high VFA peaks) might have also affected the development of commonly known electro-active microorganisms. Therefore, further studies must be carried out to identify potential extremophile electro-active bacteria, able to survive in similar conditions to the ones reported in this study.

Pictures of the GAC particles allowed verifying qualitatively that both bacteria and archaea grew attached to the particles, forming a biofilm onto their surfaces.

3.3. Possible mechanisms responsible for the AD improvement when adding GAC

The positive effect of TEs addition on AD has a known explanation: they favor microbial metabolism via synthesis of the enzymes required for VFA degradation (Banks et al., 2012). Focusing on the improved HPr degradation, this is likely to be related to the improved synthesis of formate dehydrogenase, which is responsible for formate cleavage (Banks et al., 2012). As this enzyme improves formate (and hydrogen) degradation, it leads to a thermodynamically favorable oxidation of HAc and HPr (Capson-Tojo et al., 2017b). It has been reported that the aforementioned enzyme requires Se and Mo for its synthesis (Banks et al., 2012). In addition, Co, Ni, Fe are essential in the syntrophic acetate oxidation process. This information, together with the low concentrations of Co, Mo or Ni in the FW and the inoculum, suggest that these elements (and Se) might be the most limiting TEs during AD of FW.

However, when trying to find an explanation for the positive effects of the addition of GAC on the VFA degradation, several options are feasible. The first possibility is that GAC allowed the formation of biofilms onto its surface, favoring the syntrophic interactions required for HAc and HPr degradation (Fagbohungbe et al., 2017). By decreasing the distance between the microorganisms performing MIET (using hydrogen and formate as shuttles), the reaction kinetics are accelerated and the concentrations of electron shuttles and other intermediate fermentation products (such as HAc in the case of SPO) in the media are lowered. The lower concentrations of these chemicals species would also improve the thermodynamics of SAO and SPO, making these reactions favorable. As aforementioned, another possible positive effect of GAC is the fact that it allows DIET to occur. As explained in Cruz Viggi et al. (2014), DIET improves the electron transport rates when compared to MIET. In addition, as hydrogen and formate are no longer used as electron shuttles, their

concentrations is much lower than during MIET, thus favoring the thermodynamics of SAO and SPO. Some studies using defined co-cultures have given direct evidence of DIET occurring in methanogenic communities with ethanol as substrate (Rotaru et al., 2014a; Rotaru et al., 2014b) and recent research has provided also direct evidence of DIET occurring in natural methanogenic environments (Holmes et al., 2017). However, as it is deeply discussed in Barua and Dhar (2017), due to the complex nature of the process, most of the evidence of DIET occurring in AD digesters is indirect. Using GAC to stablish electrical connections between microorganisms, different authors have reported an enhanced methanogenesis, a priori due to the occurrence of DIET. With ethanol as substrate, Liu et al. (2012) were able to reduce the lag phase in methane production. Lee et al. (2016) doubled the methane production rates from acetic acid by GAC addition, enriching the reactors with *Geobacter* sp. (known to perform DIET). Dealing with degradation of HPr, a recent study has also show that GAC addition in ethanol-stimulated batch reactors improved the syntrophic degradation of HPr and HBu, detecting and enrichment of *Geobacter* sp. in the ethanol-doped reactors (Zhao et al., 2016). Regarding complex substrates, GAC has also provided benefits in poultry blood AD, improving significantly the methane production kinetics in batch reactors (Cuetos et al., 2016). Enhanced AD kinetics have also been observed by adding GAC in a digester treating waste activated sludge, which again led to enrichments in hydrogen-utilizing microorganisms and *Geobacter* sp. (although in low abundances only up to 0.86 %). When considering the degradation of complex organic waste, Dang et al. (2017, 2016) also observed a positive effect in batch AD of dog food waste when adding GAC, with increased methane production rates and less significant VFA accumulation at higher OLRs (up to 18 kg $COD \cdot m^{-3} \cdot d^{-1}$).

Considering the aforementioned information, Figure 5 shows all the different possible

mechanisms by which GAC addition may have favored VFA degradation. Obviously, the processes described are not exclusive and all of them (or different combinations) may have occurred simultaneously.

Starting with the first possibility (syntrophic acetate and propionate oxidations as major pathways), this alternative presents a process in which DIET did not occur significantly but the syntrophic interactions were improved by biofilm formation. In the second option (acetate oxidation through DIET and syntrophic propionate oxidation), the HAc is mainly degraded by electroactive bacteria and the produced electrons are uptaked by methanogenic archaea (Lee et al., 2016). As in the first option, the HPr is mainly degraded by SPO, a pathway which is favored thermodynamically due to the DIET-mediated HAc degradation, which lowers the concentrations of hydrogen, formate or HAc in the medium. In the third possibility (syntrophic acetate oxidation and propionate degradation through DIET), HAc is degraded by SAO and HPr is degraded by DIET, performed by an electroactive microorganism able to completely oxidize this acid or to ferment it to HAc (further oxidized by SAO) (Yamada et al., 2015). Finally, the last option (4) represents the case of DIET-mediated oxidation of both HAc and HPr.

Although the analyses of the microbial communities suggest that the first option (syntrophic acetate and propionate oxidations as major pathways) was the main process taking place when GAC was added, the possibility of DIET being carried out by unidentified microorganisms cannot be discarded. In addition, DIET might have been performed even if known microorganisms were a minority (Yang et al., 2017). Further research must be performed to identify the microorganisms being an integral part of the biofilm (*i.e.* using bigger conductive particles that allow recovery of the attached biofilm), aiming at identifying potential electro-active partners thriving at the harsh conditions existing during FW AD (*i.e.* high TAN/FAN

concentrations, pH and ionic strengths).

The synergy observed when adding both GAC and TEs might have been caused by the combination of two factors: (i) the improved enzyme synthesis related to the supplementation of TEs (which enhanced the kinetics of HAc and HPr oxidation) and (ii) the favored biofilm formation (and potentially DIET occurrence) related to the addition of GAC, which enhanced VFA degradation.

The results presented suggest that GAC and TEs addition is a potential solution to stabilize industrial FW AD by favoring VFA consumption, decreasing the batch duration and thus improving significantly the methane production rates. However, if this process is to be applicable at an industrial scale both policy makers and industries must be involved. The former should aim at developing policies that favor process integration and the valorization of products (such as digestate) and the latter should focus on render the process economically feasible, optimizing its performance. More precisely, challenges such as the sources of both GAC and TEs must be addressed if a sustainable process is to be achieved (Sadhukhan et al., 2017). Production of GAC from residues, such as agricultural waste (Ioannidou and Zabaniotou, 2007), is a feasible option and waste recycled from the steel, mining and thermochemical industries are potential sustainable sources of concentrated TEs effluents (Ng et al., 2016). In addition, the application of more sustainable substitutes for both GAC and pure TEs but with similar properties (*e.g.* biochar in the case of GAC) must be pursued. Nevertheless, when using recycled materials as AD additives, the impact that these substances might have on the characteristics of the resulting digestate must always be considered if this product is to be valorized as fertilizer (*i.e.* avoid overpassing the maximum allowed TEs concentrations). Another main point to be researched to achieve a sustainable process is the in-process recycling of GAC and TEs to reduce the cost and the environmental impact of their

application (Shemfe et al., 2018). Solid-liquid separation process (with the appropriate size of filtration) coupled to the recycling of the solid phase of digestate is a potential option that could serve for GAC recycling, increasing the solids retention time in the reactors and reducing the TAN concentrations (Sadhukhan and Martinez-Hernandez, 2017). In addition, the TEs in the liquid fraction could also be concentrated (*e.g.* via flash processes) and partially recycled.

4. Conclusions

The simultaneous addition of GAC and TEs was found to favor VFA consumption and to improve the methane production kinetics and productivities. The addition of these reagents aided both syntrophic VFA oxidation and hydrogenotrophic methanogenesis. GAC sustained the growth of archaea and bacteria and enhanced syntrophic interactions, allowing higher biomass concentrations. GAC and TEs addition may be a feasible solution to stabilize FW AD by favoring VFA consumption. The identification of unknown electroactive microorganisms performing DIET in this process and the development of economically-feasible substitutes for these enhancers are two crucial factors that must be addressed in the future.

Supplementary material

E-supplementary data for this work can be found in the e-version of this article online.

Acknowledgements

The authors want to express their gratitude to Suez for financing this research under the CIFRE convention N° 2014/1146. They also acknowledge the Communauté d'Agglomération du Grand Narbonne (CAGN) for the financial support.

References

1. APHA, 2005. Standard Methods for the Examination of Water and Wastewater. American Public Health Association, Washington, DC.
2. Banks, C.J., Chesshire, M., Heaven, S., Arnold, R., 2011. Anaerobic digestion of source-segregated domestic food waste: Performance assessment by mass and energy balance. Bioresour. Technol. 102, 612–620.
3. Banks, C.J., Chesshire, M., Stringfellow, A., 2008. A pilot-scale trial comparing mesophilic and thermophilic digestion for the stabilisation of source segregated kitchen waste. Water Sci. Technol. 58, 1475–1481.
4. Banks, C.J., Zhang, Y., Jiang, Y., Heaven, S., 2012. Trace element requirements for stable food waste digestion at elevated ammonia concentrations. Bioresour. Technol. 104, 127–135.
5. Barua, S., Dhar, B.R., 2017. Advances Towards Understanding and Engineering Direct Interspecies Electron Transfer in Anaerobic Digestion. Bioresour. Technol. 244, 698-707.
6. Batstone, D.J., Keller, J., Angelidaki, I., Kalyuzhny, S. V, Pavlostathis, S.G., Rozzi, A., Sanders, W.T.M., Siegrist, H., Vavilin, V.A., 2002. Anaerobic digestion model no. 1 (ADM1). IWA Publishing.
7. Capson-Tojo, G., Rouez, M., Crest, M., Steyer, J.-P., Delgenès, J.-P., Escudié, R., 2016. Food waste valorization via anaerobic processes: a review. Rev. Env. Sci. Biotechnol. 15, 499–547.
8. Capson-Tojo, G., Rouez, M., Crest, M., Trably, E., Steyer, J., Bernet, N., Delgenès, J., Escudié, R., 2017a. Kinetic study of dry anaerobic co-digestion of food waste and cardboard for methane production. Waste Manag. 69, 470–479.
9. Capson-Tojo, G., Ruiz, D., Rouez, M., Crest, M., Steyer, J.-P., Bernet, N., Delgenès, J.-P., Escudié, R., 2017b. Accumulation of propionic acid during consecutive batch anaerobic digestion of commercial food waste. Bioresour. Technol. 245, 724–733.
10. Capson-Tojo, G., Trably, E., Rouez, M., Crest, M., Steyer, J.-P., Delgenès, J.-P., Escudié, R., 2017c. Dry anaerobic digestion of food waste and cardboard at different substrate loads, solid contents and co-digestion proportions. Bioresour. Technol. 233, 166–175.
11. Cruz Viggi, C., Rossetti, S., Fazi, S., Paiano, P., Majone, M., Aulenta, F., 2014. Magnetite particles triggering a faster and more robust syntrophic pathway of methanogenic propionate degradation. Environ. Sci. Technol. 48, 7536–7543.
12. Cuetos, M.J., Martinez, E.J., Moreno, R., Gonzalez, R., Otero, M., Gomez, X., 2016. Enhancing anaerobic digestion of poultry blood using activated carbon. J. Adv. Res. 297–307.
13. Dang, Y., Holmes, D.E., Zhao, Z., Woodard, T.L., Zhang, Y., Sun, D., Wang, L.-Y., Nevin, K.P., Lovley, D.R., 2016. Enhancing anaerobic digestion of complex organic waste with carbon-based conductive materials. Bioresour. Technol. 220, 516–522.

14. Dang, Y., Sun, D., Woodard, T.L., Wang, L.-Y., Nevin, K.P., Holmes, D.E., 2017. Stimulation of the anaerobic digestion of the dry organic fraction of municipal solid waste (OFMSW) with carbon-based conductive materials. Bioresour. Technol. 238, 30–38.

15. Dubois, M., Gilles, K.A., Hamilton, J.K., Rebers, P.A., Smith, F., 1956. Colorimetric Method for Determination of Sugars and Related Substances. Anal. Chem. 28, 350–356.

16. Fagbohungbe, M.O., Herbert, B.M.J., Hurst, L., Ibeto, C.N., Li, H., Usmani, S.Q., Semple, K.T., 2017. The challenges of anaerobic digestion and the role of biochar in optimizing anaerobic digestion. Waste Manag. 61, 236–249.

17. Fisgativa, H., Tremier, A., Le Roux, S., Bureau, C., Dabert, P., 2017. Understanding the anaerobic biodegradability of food waste: Relationship between the typological, biochemical and microbial characteristics. J. Environ. Manag. 188, 95–107.

18. Holmes, D.E., Shrestha, P.M., Walker, D.J.F., Dang, Y., Nevin, K.P., Woodard, T.L., Lovley, D.R., 2017. Metatranscriptomic evidence for direct interspecies electron transfer between Geobacter and Methanothrix species in methanogenic rice paddy soils. Applied Environ. Microbiol. 83.

19. Ioannidou, O. and Zabaniotou, A., 2007. Agricultural residues as precursors for activated carbon production—a review. Renew. Sustain. Energy Rev., 11, 1966-2005.

20. Jiang, Y., Banks, C., Zhang, Y., Heaven, S., Longhurst, P., 2017. Quantifying the percentage of methane formation via acetoclastic and syntrophic acetate oxidation pathways in anaerobic digesters. Waste Manag. 71, 749-756.

21. Jimenez, J., Vedrenne, F., Denis, C., Mottet, A., Déléris, S., Steyer, J.-P., Rivero, J.A.C., 2013. A statistical comparison of protein and carbohydrate characterisation methodology applied on sewage sludge samples. Water Res. 47, 1751–1762.

22. Lee, J.Y., Lee, S.H., Park, H.D., 2016. Enrichment of specific electro-active microorganisms and enhancement of methane production by adding granular activated carbon in anaerobic reactors. Bioresour. Technol. 205, 205–212.

23. Liu, F., Rotaru, A.-E., Shrestha, P.M., Malvankar, N.S., Nevin, K.P., Lovley, D.R., 2012. Promoting direct interspecies electron transfer with activated carbon. Energy Environ. Sci. 5, 8982.

24. Lovley, D.R., 2017. Syntrophy Goes Electric: Direct Interspecies Electron Transfer. Annu. Rev. Microbiol. 71, 643-664.

25. Maus, I., Wibberg, D., Stantscheff, R., Eikmeyer, F.G., Seffner, A., Boelter, J., Szczepanowski, R., Blom, J., Jaenicke, S., König, H., Pühler, A., Schlüter, A., 2012. Complete genome sequence of the hydrogenotrophic, methanogenic archaeon Methanoculleus bourgensis strain MS2T, isolated from a sewage sludge digester. J. Bacteriol. 194, 5487–5488.

26. Moscoviz, R., de Fouchécour, F., Santa-Catalina, G., Bernet, N., Trably, E., 2017. Cooperative growth of Geobacter sulfurreducens and Clostridium pasteurianum with subsequent metabolic shift in glycerol fermentation. Sci. Rep. 7, 44334.

27. Motte, J.-C., Escudié, R., Beaufils, N., Steyer, J.-P., Bernet, N., Delgenès, J.-P., Dumas, C., 2014. Morphological structures of wheat straw strongly impacts its anaerobic

digestion. Ind. Crops Prod- 52, 695–701.

28. Motte, J.-C., Trably, E., Escudié, R., Hamelin, J., Steyer, J.-P., Bernet, N., Delgenes, J.-P., Dumas, C., 2013. Total solids content: a key parameter of metabolic pathways in dry anaerobic digestion. Biotechnol. biofuels 6, 164.

29. Nakamura, K., Takahashi, A., Mori, C., Tamaki, H., Mochimaru, H., Nakamura, K., Takamizawa, K., Kamagata, Y., 2013. Methanothermobacter tenebrarum sp. nov., a hydrogenotrophic, thermophilic methanogen isolated from gas-associated formation water of a natural gas field. Int. J. System. Evol. Microbiol. 63, 715–722.

30. Ng, K.S., Head, I., Premier, G.C., Scott, K., Yu, E., Lloyd, J., Sadhukhan, J., 2016. A multilevel sustainability analysis of zinc recovery from wastes. Resour. Conserv. Recycl., 113, 88-105

31. Qiang, H., Lang, D.-L., Li, Y.-Y., 2012. High-solid mesophilic methane fermentation of food waste with an emphasis on Iron, Cobalt, and Nickel requirements. Bioresour. Technol. 103, 21–7.

32. Qiang, H., Niu, Q., Chi, Y., Li, Y., 2013. Trace metals requirements for continuous thermophilic methane fermentation of high-solid food waste. Chem. Eng. J. 222, 330–336.

33. Rajagopal, R., Massé, D.I., Singh, G., 2013. A critical review on inhibition of anaerobic digestion process by excess ammonia. Bioresour. Technol. 143, 632–641.

34. Rotaru, A.-E., Shrestha, P.M., Liu, F., Shrestha, M., Shrestha, D., Embree, M., Zengler, K., Wardman, C., Nevin, K.P., Lovley, D.R., 2014. A new model for electron flow during anaerobic digestion: direct interspecies electron transfer to Methanosaeta for the reduction of carbon dioxide to methane. Energy Environ. Sci. 7, 408–415.

35. Rotaru, A.E., Shrestha, P.M., Liu, F., Markovaite, B., Chen, S., Nevin, K.P., Lovley, D.R., 2014. Direct interspecies electron transfer between Geobacter metallireducens and Methanosarcina barkeri. Appl. Environ. Microbiol. 80, 4599–4605.

36. Roy, F., Samain, E., Dubourguier, H.C., Albagnac, G., 1986. Synthrophomonas sapovorans sp. nov., a new obligately proton reducing anaerobe oxidizing saturated and unsaturated long chain fatty acids. Arch. Microbiol. 145, 142–147.

37. Savant, D. V., Shouche, Y.S., Prakash, S., Ranade, D.R., 2002. Methanobrevibacter acididurans sp. nov., a novel methanogen from a sour anaerobic digester. International J. System. Evol. Microbiol. 52, 1081–1087.

38. Sadhukhan, J., Ng, K.S. and Martinez Hernandez E., 2014. Biorefineries and chemical processes: design, integration and sustainability analysis. John Wiley & Sons.

39. Sadhukhan, J., Joshi, N., Shemfe, M. and Lloyd, J.R., 2017. Life cycle assessment of sustainable raw material acquisition for functional magnetite bionanoparticle production. J. Environ. Manag., 199, 116-125.

40. Sadhukhan, J. and Martinez-Hernandez, E., 2017. Material flow and sustainability analyses of biorefining of municipal solid waste. Bioresour. Technol., 243, 135-146.

41. Shemfe, M., Gadkari, S., Yu, E., Rasul, S., Scott, K., Head, I., Gu, S. and Sadhukhan, J., 2018. Life cycle, techno-economic and dynamic simulation assessment of bioelectrochemical systems: A case of formic acid synthesis. Bioresour. Technol., 255,

39-49.

42. Voelklein, M.A., O'Shea, R., Jacob, A., Murphy, J.D., 2017. Role of trace elements in single and two-stage digestion of food waste at high organic loading rates. Energy 121, 185-192.

43. Wu, X.Y., Shi, K.L., Xu, E.W., Wu, M., Oren, A., Zhu, X.F., 2010. Alkaliphilus halophilus sp. nov., a strictly anaerobic and halophilic bacterium isolated from a saline lake, and emended description of the genus Alkaliphilus. Int. J. System. Evol. Microbiol. 60, 2898–2902.

44. Yamada, C., Kato, S., Ueno, Y., Ishii, M., Igarashi, Y., 2015. Conductive iron oxides accelerate thermophilic methanogenesis from acetate and propionate. J. Biosci. Bioeng. 119, 678–682.

45. Yang, Y., Zhang, Y., Li, Z., Zhao, Z., Quan, X., Zhao, Z., 2017. Adding granular activated carbon into anaerobic sludge digestion to promote methane production and sludge decomposition. J. Clean Prod. 149, 1101–1108.

46. Zhang, L., Lee, Y.-W., Jahng, D., 2011. Anaerobic co-digestion of food waste and piggery wastewater: Focusing on the role of trace elements. Bioresour. Technol. 102, 5048–5059.

47. Zhang, W., Wu, S., Guo, J., Zhou, J., Dong, R., 2015a. Performance and kinetic evaluation of semi-continuously fed anaerobic digesters treating food waste: role of trace elements. Bioresour. Technol, 178, 297–305.

48. Zhang, W., Zhang, L., Li, A., 2015b. Enhanced anaerobic digestion of food waste by trace metal elements supplementation and reduced metals dosage by green chelating agent [S, S]-EDDS via improving metals bioavailability. Water Res. 84, 266–77.

49. Zhao, Z., Zhang, Y., Yu, Q., Dang, Y., Li, Y., Quan, X., 2016. Communities stimulated with ethanol to perform direct interspecies electron transfer for syntrophic metabolism of propionate and butyrate. Water Res. 102, 475–484.

Figure and table captions

Figure 1. Evolution of the (A) methane yields, (B) total products obtained (g COD), and concentrations of (C) acetic, (D) propionic, (E) butyric and (F) valeric acids during the first feeding (~ 30 g VS FW·l^{-1})

Figure 2. Evolution of the (A) methane yields, (B) total products obtained (g COD) and concentrations of (C) acetic, (D) propionic, (E) butyric and (F) valeric acids during the second feeding (~ 30 g VS FW·l^{-1})

Figure 3. Sequencing and qPCR results for the archaea (above) and the bacteria (below) in the food waste and in the reactors. The days indicate the moment of the batch when the samples were taken

Figure 4. Growth rates of bacteria in the (A) Control reactors, (B) TEs reactors and (C) GAC reactors during the first batch. The colors represent the orders shown in Figure 3. OTU stands for operational taxonomic unit

Figure 5. Possible mechanisms of VFA degradation favored by the addition of GAC: (1)

syntrophic acetate and propionate oxidations, (2) acetate oxidation through DIET and syntrophic propionate oxidation, (3) syntrophic acetate oxidation and propionate degradation through DIET and (4) acetate and propionate oxidations through DIET

Figure S1. Evolution of the methane production rates during the first feed in the reactor supplemented with GAC (GAC) and the reactor supplemented with GAC and inoculated with *Geobacter sulfurreducens* (GAC + Geo). Each condition was carried out in triplicate

Figure S2. Evolution of the (A) methane production rates and the (B) concentrations of propionic acid during the third feeding (~ 55 g VS $FW \cdot l^{-1}$)

Figure S3. Microscopy pictures of a GAC particle taken after DAPI coloration (left) and at 420 nm (right). Each picture represents a total length of 50 µm. The presence of bacterial and archaeal cells attached onto the GAC particles was qualitatively assessed using coloration and fluorescence microscopy. DNA was colored using DAPI (4',6-diamino-2-fenilindol). A diluted digestate sample was mixed with the DAPI solution (25 $\mu g \cdot ml^{-1}$) at a volumetric ratio of 19:1 and the mixture was incubated at ambient temperature for 20 min. The natural fluorescence of methanogenic archaea at 420 nm (due to the coenzyme F_{420}) was used for their observation. To avoid crushing the GAC particles (and thus the biofilm), the samples were fixed in agar (1.5 % in Tris pH 7.5 0.1M) while it was still liquid and covered with a layer of Milli-Q water (around 1 mm deep). A submergible lens (Olympus UM Plan FLN 60x/1.00) coupled to a microscope Olympus BX53, a motorized reflected fluorescence system (Olympus BX3-RFAA) and a control box (Olympus U-CBM) was used

Table 1. Maximum methane production rates, COD recoveries and final pH values obtained after the first feeding (Batch # 1) and the second feeding (Batch # 2). The maximum consumptions rates of acetic and propionic acids and the times required for total VFA consumption are also shown

Table 2. Concentrations of TAN and FAN and ionic strengths in the reactors after the second feeding

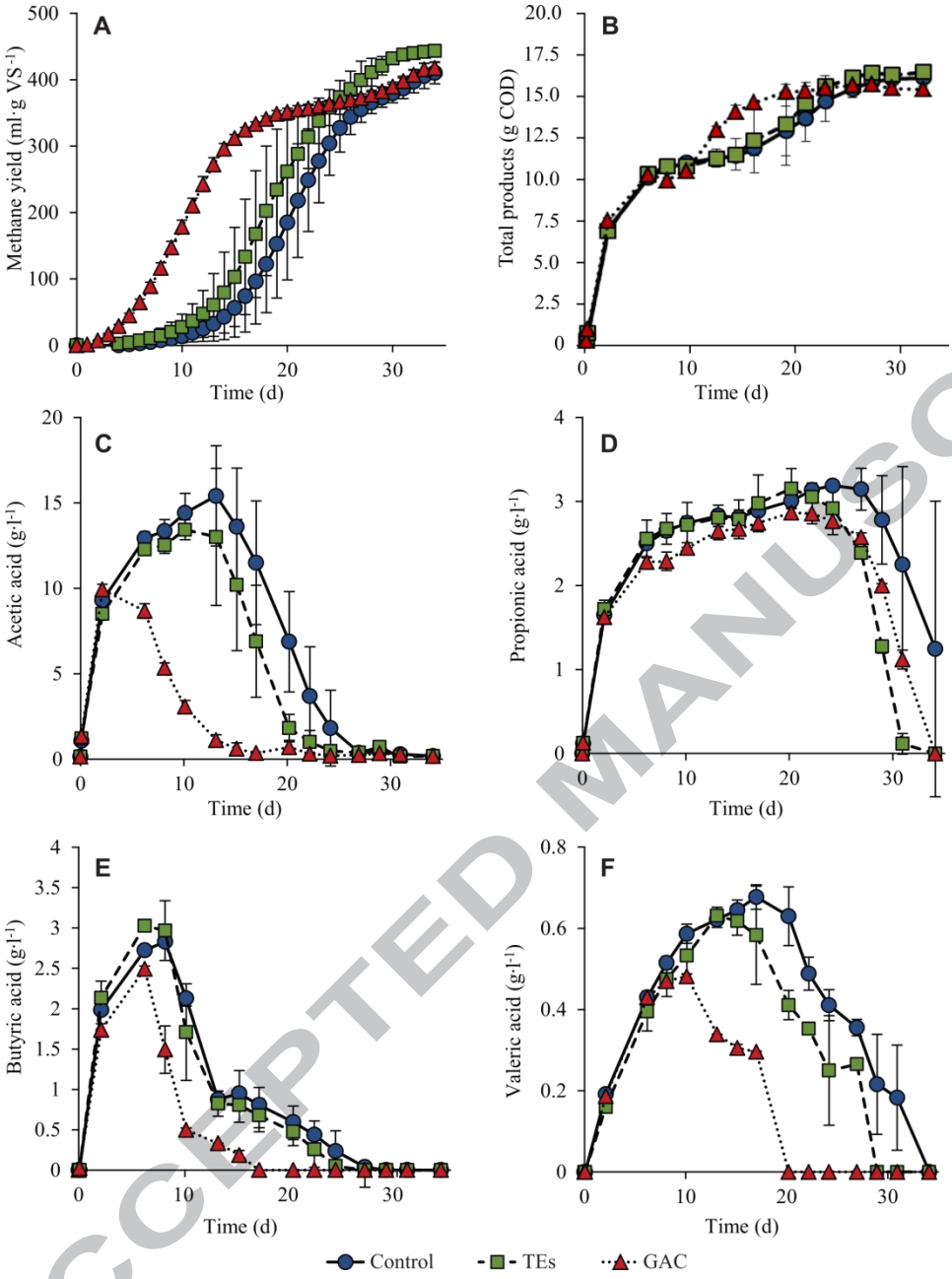

Figure 1. Evolution of the (A) methane yields, (B) total products obtained (g COD), and concentrations of (C) acetic, (D) propionic, (E) butyric and (F) valeric acids during the first feeding (~ 30 g VS FW·l^{-1})

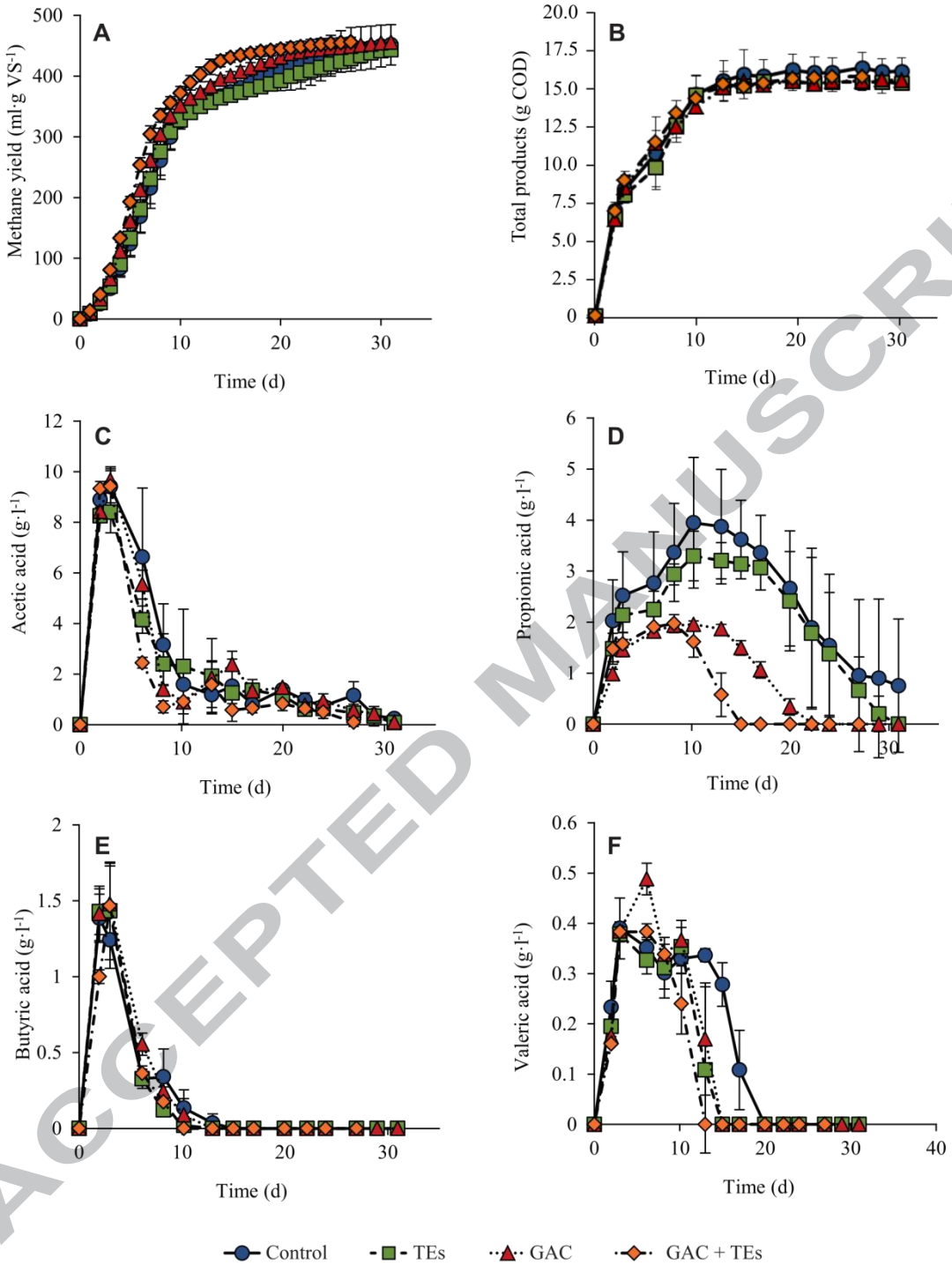

Figure 2. Evolution of the (A) methane yields, (B) total products obtained (g COD) and concentrations of (C) acetic, (D) propionic, (E) butyric and (F) valeric acids during the second feeding (~ 30 g VS FW·l^{-1})

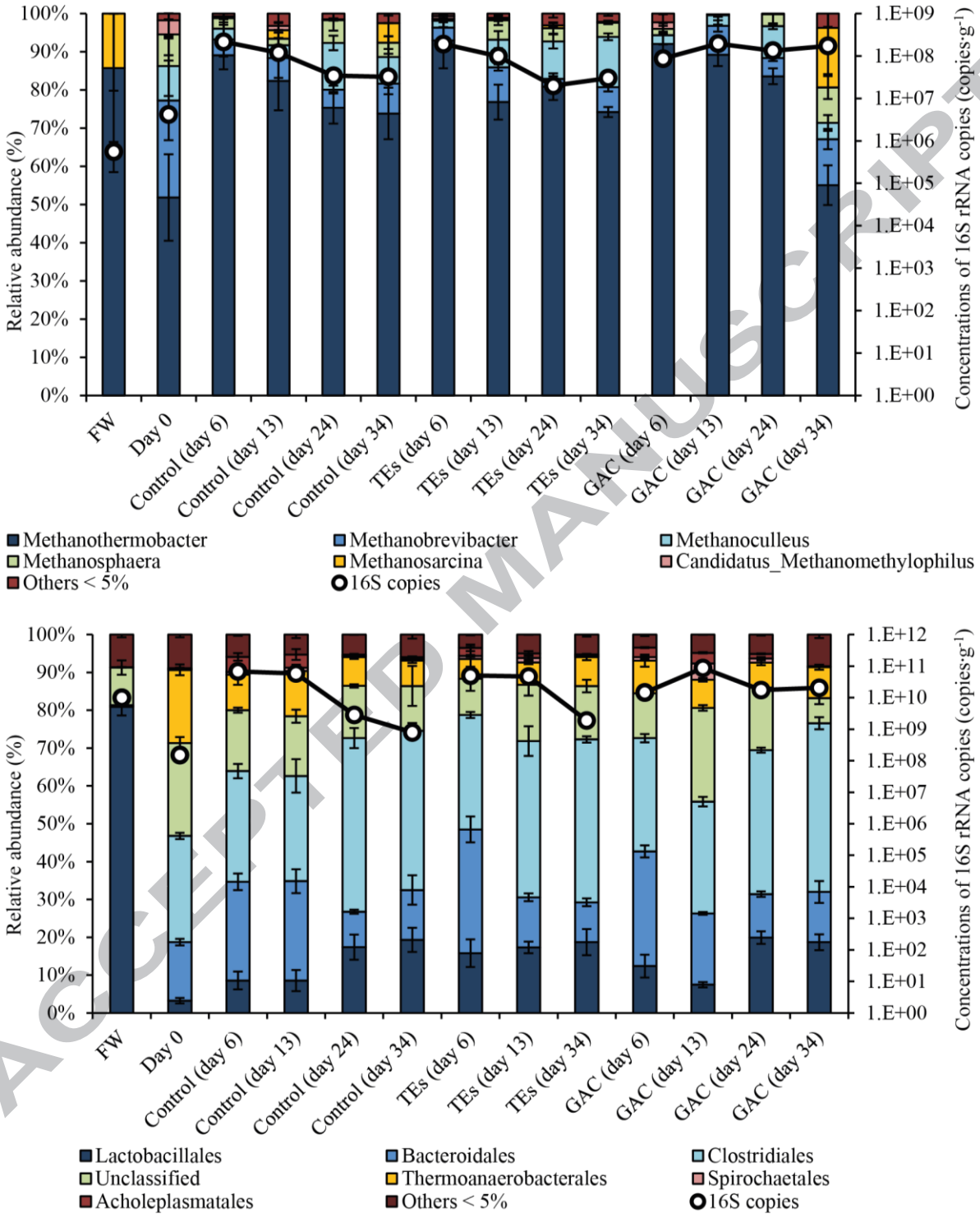

Figure 3. Sequencing and qPCR results for the archaea (above) and the bacteria (below) in the food waste and in the reactors. The days indicate the moment of the batch when the samples were taken

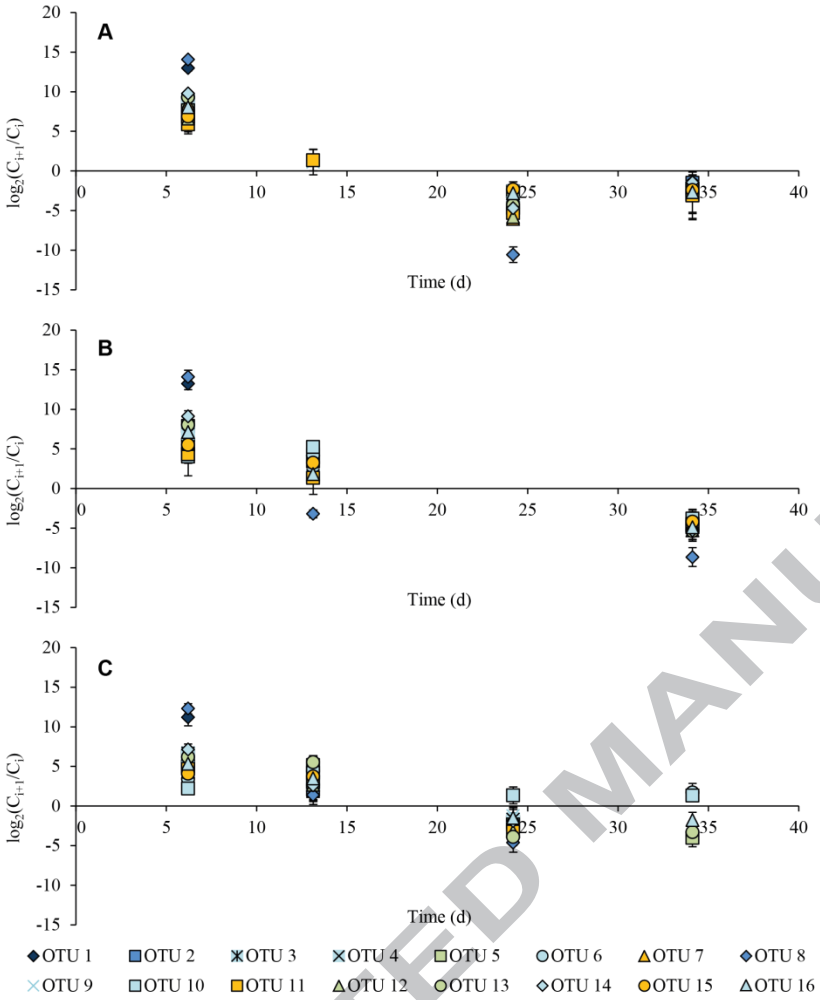

OTU	Class	Order	Family	Genus
1	Bacilli	Lactobacillales	Unclassified	Unclassified
2	Bacteroidia	Bacteroidales	Porphyromonadaceae	Proteiniphilum
3	Clostridia	Clostridiales	Unclassified	Unclassified
4	Clostridia	Clostridiales	Clostridiaceae_1	Clostridium_sensu_stricto_1
5	Spirochaetes	Unclassified	Unclassified	Unclassified
6	Clostridia	Clostridiales	Clostridiaceae_2	Alkaliphilus
7	Clostridia	Thermoanaerobacterales	Thermoanaerobacteraceae	Gelria
8	Bacteroidia	Bacteroidales	Bacteroidaceae	Bacteroides
9	Clostridia	Clostridiales	Syntrophomonadaceae	Unclassified
10	Clostridia	Clostridiales	Syntrophomonadaceae	Syntrophomonas
11	Clostridia	Thermoanaerobacterales	Thermoanaerobacteraceae	Gelria
12	OPB54	Unclassified	Unclassified	Unclassified
13	OPB54	Unclassified	Unclassified	Unclassified
14	Clostridia	Clostridiales	Family_XI	Unclassified
15	Clostridia	Thermoanaerobacterales	Thermoanaerobacteraceae	Syntrophaceticus
16	Clostridia	Clostridiales	Family_XI	Tissierella

Figure 4. Growth rates of bacteria in the (A) Control reactors, (B) TEs reactors and (C) GAC reactors during the first batch. The colors represent the orders shown in Figure 3. OTU stands for operational taxonomic unit

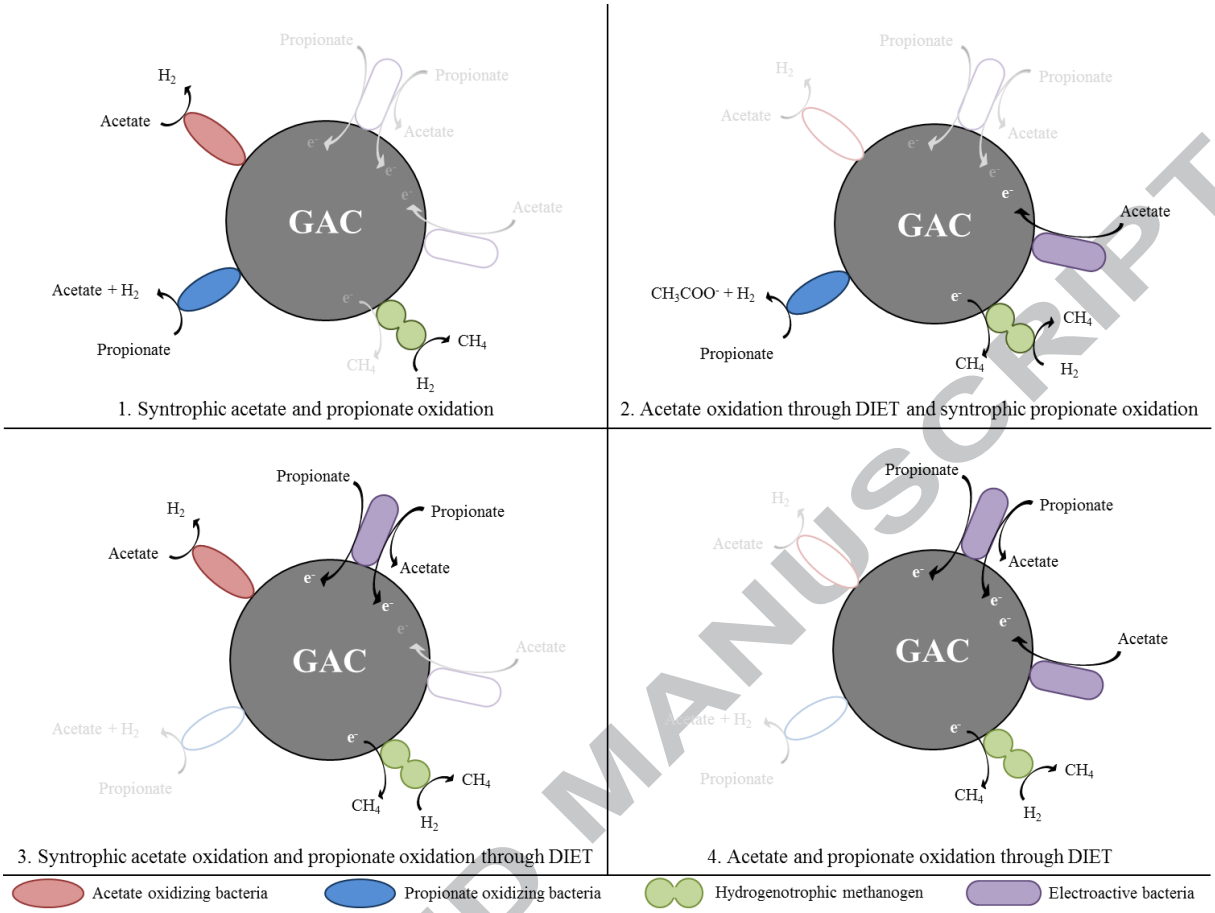

Figure 5. Possible mechanisms of VFA degradation favored by the addition of GAC: (1) syntrophic acetate and propionate oxidations, (2) acetate oxidation through DIET and syntrophic propionate oxidation, (3) syntrophic acetate oxidation and propionate degradation through DIET and (4) acetate and propionate oxidations through DIET

Table 1. Maximum methane production rates, COD recoveries and final pH values obtained after the first feeding (Batch # 1) and the second feeding (Batch # 2). The maximum consumptions rates of acetic and propionic acids and the times required for total VFA consumption are also shown

Reactor & batch #	Maximum CH_4 production rate ($ml \cdot d^{-1}$)	Final COD recovery (%)[1]	Final pH	Maximum HAc consumption rate ($g \cdot l^{-1} \cdot d^{-1}$)	Maximum HPr consumption rate ($g \cdot l^{-1} \cdot d^{-1}$)	Time for HAc (d)[2]	Time for HPr (d)	Time for HBu (d)	Time for HVal (d)
Control 1	397 ± 66	86.0 ± 1.60	8.13 ± 0.02	1.59 ± 0.13	0.32 ± 0.19	27	> 34[3]	29	34
TEs 1	419 ± 27	87.9 ± 0.01	8.12 ± 0.01	1.76 ± 0.32	0.58 ± 0.10	24	31	27	29
GAC 1	406 ± 3	81.9 ± 0.40	8.13 ± 0.01	1.74 ± 0.07	0.44 ± 0.04	15	34	17	20
Control 2	545 ± 58	92.0 ± 2.37	8.12 ± 0.02	1.68 ± 1.98	0.35 ± 0.23	10	> 31[3]	15	20
TEs 2	584 ± 14	88.7 ± 2.01	8.12 ± 0.03	1.35 ± 0.29	0.28 ± 0.23	10	31	13	15
GAC 2	600 ± 31	90.7 ± 0.74	8.11 ± 0.01	2.01 ± 0.32	0.24 ± 0.00	8	22	13	15
GAC + TEs 2	719 ± 14	90.7 ± 1.58	8.03 ± 0.03	2.22 ± 0.28	0.37 ± 0.05	8	15	10	13

1. Calculated considering the input COD coming from the FW and the COD recovered as final AD products (*i.e.* methane and VFAs)
2. As the acetic acid was also a product of the degradation of other acids, the times shown correspond to the first moment with concentrations lower than 2 $g \cdot l^{-1}$
3. Total consumption not achieved

TEs stands for trace elements, GAC for granular activated carbon, HAc for acetic acid, HPr for propionic acid, HBu for butyric acid and HVal for valeric acid

Table 2. Concentrations of TAN and FAN and ionic strengths in the reactors after the second feeding

Reactor	Ionic strength (M)	TAN ($g \cdot l^{-1}$)	FAN ($mg \cdot l^{-1}$)
Control	0.56 ± 0.01	11.1 ± 0.5	1102 ± 133
TEs	0.57 ± 0.07	11.7 ± 0.8	1067 ± 10
GAC	0.47 ± 0.06	10.0 ± 0.7	971 ± 8
GAC + TEs	0.45 ± 0.01	10.2 ± 0.2	878 ± 11

TAN stands for total ammonia nitrogen and FAN for free ammonia nitrogen

Graphical abstract

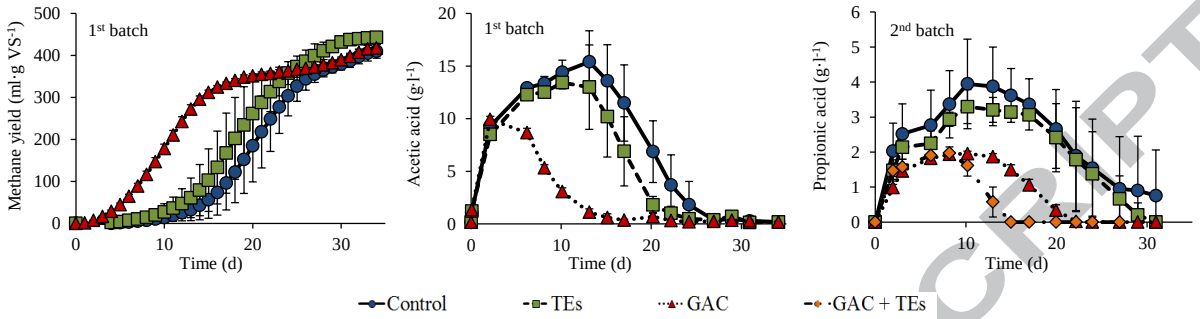

- 1st batch: FW AD kinetics improved by GAC addition due to favored biomass acclimation; TEs favored propionate degradation
- 2nd batch: synergy observed when dosing GAC and TEs simultaneously; enhanced propionate degradation

FW stands for food waste, AD for anaerobic digestion, GAC for granular activated carbon and TEs for trace elements

Highlights

- High methane yields achieved: 410-456 ml $CH_4 \cdot g\ VS^{-1}$
- Granular activated carbon favors biomass acclimation and microbial growth
- Granular activated carbon and trace elements favored propionate degradation
- Synergy observed when adding both substances simultaneously
- Average daily methane productivities doubled (up to 348 ml $CH_4 \cdot l^{-1}$)